

Supplementary Information

Layer-Controlled Continuous MoS₂ Growth using Spin-Coatable Metal Precursor Buffer

Dong Hwan Kim,^{a,†} Jinyoung Seo,^{b,†} Yoonbeen Kang,^b Bumjun Lee,^b and Sang-Yong Ju^{a,b,}*

^a Graduate Program of Semiconductor Science and Engineering, Yonsei University, Seoul 03722, Republic of Korea; ^b Department of Chemistry, Yonsei University, Seoul 03722, Republic of Korea

[†] Equally contributed to this work.

*To whom correspondence should be addressed; E-mail: syju@yonsei.ac.kr

Note S1: Full explanation of Fig. S1

The formation of uniform MoS₂ films through CVD growth is significantly influenced by the hydrophilicity of the substrate, which enables uniform hydrogen bonds with metal precursor adsorbates. AFM measurements were first conducted on both O₂ plasma-treated and untreated (bare) 285 nm-thick SiO₂/Si substrates. The resulting AFM height profiles (Fig. S1b–S1c) indicate that the surface topographies are comparable, with both substrates exhibiting an average surface roughness ($\langle R \rangle$) of approximately 0.2 nm. Measurements of water droplet contact angles (Fig. S1d) indicated that the O₂ plasma-treated substrate is hydrophilic (8.5°) compared to a non-treated bare substrate (73.3°). Fig. S1a shows the optical image of a hydrophilic patterned CVD-grown MoS₂ sample. This sample was prepared after the CVD step using a cross-marked hydrophilic patterned substrate, achieved by O₂-plasma treatment with a metal shadow mask (inset), followed by spin-coating the MoO₃/SC solution over the entire substrate (see Methods). The O₂ plasma-treated region exhibits different optical contrasts compared to the untreated areas.

High-magnification optical images (Fig. S1e–S1f) reveal that untreated areas show presumably MoO₃ particles, whereas O₂ plasma-treated regions form a continuous MoS₂ film. Raman spectra (Fig. S1g) confirm that the treated region displays the characteristic E_{2g}¹ and A_{1g} bands of MoS₂ at 384.9 and 405.9 cm⁻¹, respectively, with a peak separation of 21.0 cm⁻¹ indicating SL or BL MoS₂. The deconvoluted band at 375.1 cm⁻¹ (purple) corresponds to a defective longitudinal optical (LO) mode. These results highlight that a hydrophilic substrate supports continuous MoS₂ growth through MoO₃/SC spin-coating, while a hydrophobic substrate leads to particle aggregation. The hydrophilic region retains its pattern from spin-coating to CVD growth, demonstrating patterned MoS₂ film formation.

Note S2: Full explanation of Fig. S4a–S4d

XPS measurements were conducted to investigate the chemical states of sodium and SC. For this purpose, a $\text{Na}_2\text{MoO}_4/\text{SC}$ dispersion drop-cast on 285 nm-thick SiO_2/Si substrate (namely $\text{Na}_2\text{MoO}_4/\text{SC}$ drop-cast) and a MoS_2 film were analyzed alongside as-received powders of SC, MoO_3 , and Na_2MoO_4 . The offset, normalized XPS survey spectra of these five samples are shown in Fig. S4a. These spectra reflect the relative sensitivity factor and electron counts of each orbital. Key regions of interest—S $2p$, Mo $3d$, and Na $1s$ —are highlighted. It is also noteworthy that all samples, including MoO_3 and Na_2MoO_4 , exhibit adventitious carbon in their spectra.

Fig. S4b represents the detailed S $2p$ spectra. Only the MoS_2 sample displays a spin-orbit doublet corresponding to S $2p_{3/2}$ and S $2p_{1/2}$ at binding energies of 161.1 and 162.2 eV, respectively, consistent with the value reported for powder-phase MoS_2 .¹ Fig. S4c represents the detailed Mo $3d$ spectra. No Mo signal is detected for SC, whereas MoO_3 , Na_2MoO_4 , and the drop-cast samples exhibit a spin-orbit doublet arising from Mo^{6+} (Mo $3d_{5/2}$ and Mo $3d_{3/2}$), confirming the Mo(VI) oxidation state. In contrast, the MoS_2 film features three distinct peaks: a Mo^{4+} spin-orbit doublet at 228.2 eV ($3d_{5/2}$) and 231.3 eV ($3d_{3/2}$) with 3.1 eV separation, and an additional singlet peak at 225.3 eV corresponding to S $2s$ —characteristic of 2H phase MoS_2 .²

Lastly, Fig. S4d display the detailed Na $1s$ spectra. Except for MoO_3 , which lacks a significant sodium signal, all other samples exhibit well-defined Na peaks. These peaks show a progressive blue shift in binding energy, ranging from 1070.2 eV in SC to 1071.4 eV in the MoS_2 film. The Na $1s$ peak at 1071.4 eV corresponds to neutral sodium, as expected for elemental sodium.³ In comparison, powdery Na_2MoO_4 and $\text{Na}_2\text{MoO}_4/\text{SC}$ drop-coat samples show a 0.4 eV blue shift, consistent with observations from spin-coated Na_2MoO_4 .⁴

Note S3: Full explanation of Fig. S5–S7

In the MoO_3 only case, although spin-coating was successful on the O_2 -plasma treated substrate, the half spin-coated sample exhibits that slight darkening of optical contrast occurs across several positions in optical images during the exposure to constant T_{CVD} at 800°C over 10 min. (Fig. S5b–S5d). Furthermore, C_{R} trends of positions 1, 2, and 3 exhibit weak exponential changes much below the SL region (Fig. S5e), indicating discontinuous formation of MoS_2 if any. The optical image (Fig. S5f) shows that the spin-coat area possesses contrast presumably owing to MoO_3 and MoS_2 . Raman spectra exhibit that only the interfacial position exhibits weak and characteristic MoS_2 bands at ~ 385.8 and $\sim 405.5\text{ cm}^{-1}$, indicating SL MoS_2 , while other positions, such as 2 and 3 do not show any bands except for Si bands. This result indicates that the in situ formation of sodium from the SC plays a role in the formation of a continuous MoS_2 at low temperatures.

For the case of Na_2MoO_4 without SC, we observed the formation of discontinuous ML MoS_2 from a 10 mM Na_2MoO_4 solution, consistent with the literature.⁵ First, as shown in Fig. S6a, overall t_{rxn} requires much longer time over 20 min at 800°C . A series of optical images (Fig. S6b–S6d) display a slight darkening of the uniformly spin-coated area over t_{rxn} . Furthermore, C_{R} trends of positions 1, 2, and 3 (Fig. S6e) show slow changes from 0 to 7, which is much below SL C_{R} region. Unlike the case of MoO_3 only, positions farther away from the interface are much darker. To check the growth in the central region of the spin-coat, the optical image (Fig. S6f) displays that discontinuous micrometer-sized grains are grown. Raman spectra exhibit that while the other positions indicated in Fig. S6b and S6f do not show characteristic MoS_2 peaks, positions 3 and 4 shows $\text{E}^1_{2\text{g}}$ and A^1_{lg} bands of MoS_2 . Position 4 shows two bands at 383.6 and 409.8 cm^{-1} (interpeak separation: 26.2 cm^{-1}), indicating ML MoS_2 , whereas position 3 displays 388.0 and 407.7 cm^{-1} (interpeak separation: 19.7 cm^{-1}), indicating SL MoS_2 . This result indicates that Na_2MoO_4

compared to $\text{Na}_2\text{MoO}_4/\text{SC}$ promotes localized ML MoS_2 across the sample. This also indicates that uniform coating alone cannot explain the uniform continuous growth of MoS_2 promoted by $\text{Na}_2\text{MoO}_4/\text{SC}$. This might be related to the porous structure of sodium catalyst promoted by SC.⁶

For the case of MoO_3 with SDS, which is a well-known dispersant, similar growth behavior to the case of MoO_3 without SC was witnessed, considering the interfacial formation of MoS_2 : although the initial spin-coating of MoO_3/SDS dispersion was successful, the subsequent sulfurization of the precursor did not lead to the formation of a continuous MoS_2 . Along the growth parameter change over 10 min from 400 to 800 °C (Fig. S7a), a series of optical images (Fig. S7b–S7d) shows a lightened contrast trend and similar contrast between the spin-coat and the bare areas at the end, presumably due to the decomposition (or sublimation) of SDS. Quantitative C_R trend (Fig. S7e) of each position indicated in (Fig. S7b) also shows changes from 8 to near 0. This indicates that desorption of the MoO_3/SDS spin-coat occurs. The optical image of the central area from the spin-coat (Fig. S7f) does not show any noticeable feature. Raman spectra (Fig. S7g) of the interface and center exhibit no MoS_2 bands except for the position 1 which is the interface. This indicates that sodium-containing dispersant alone cannot explain the formation of MoS_2 . The $\text{p}K_a$ of hydrogensulfate in the SDS is ~ 2 , which is strongly acidic. Therefore, the cation exchange between H_2MoO_4 and sodium of the sulfate group in SDS is prohibited. The dispersant having buffer capability at mildly acidic conditions would be an appropriate choice for future research.

Fig. S1 Substrate hydrophilicity effect on MoS₂ formation. (a) Optical images of patterned MoS₂ film formation via CVD growth after O₂-plasma treatment of a bare substrate using a metal shadow mask (inset), followed by spin-coating with a 6 mM MoO₃/SC solution. The pattern exhibits non-distinct boundaries, likely due to reactive ion diffusion at the interface of the shadow metal mask. (b–c) AFM height images of (b) O₂ plasma-treated and (c) bare 285 nm-thick SiO₂/Si substrates. Average surface roughness <R> is provided. (d) Water contact angle comparison between (top) O₂ plasma-treated and (bottom) untreated substrates. High-magnification optical images of (e) the O₂ plasma-treated area and (f) the untreated area. (g) Offset Raman spectra of (top) the O₂ plasma-treated area and (bottom) the untreated area. The spectrum was deconvoluted using Lorentzian fittings. Experimental data are shown with empty circles, and the red curve represents the sum of each Lorentzian peak.

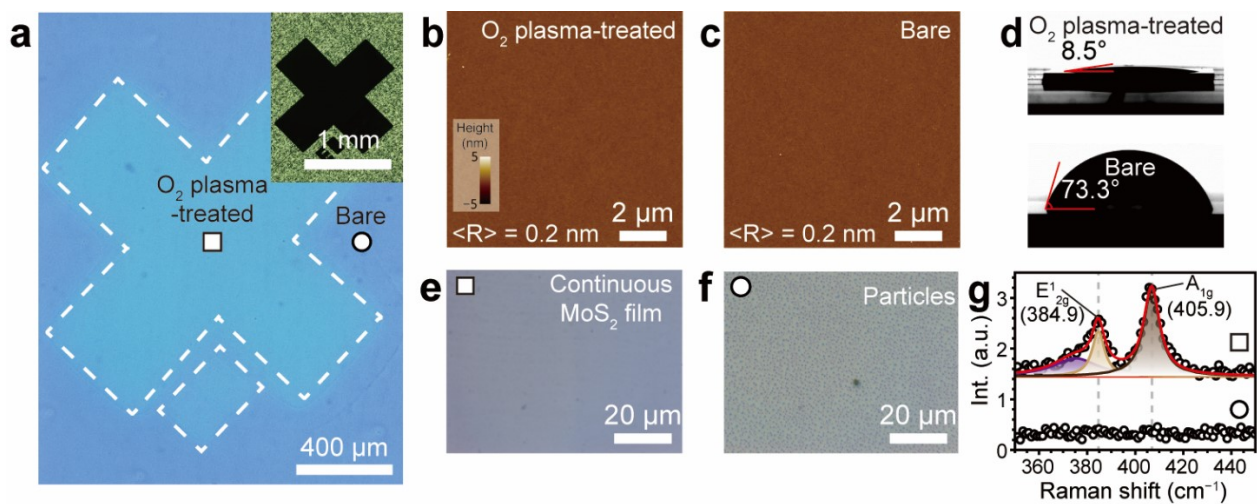


Fig. S2 Comparison of offset AFM height profiles. (a) Offset AFM height profiles of $\text{Na}_2\text{MoO}_4/\text{SC}$ spin-coats as a function of $\text{Na}_2\text{MoO}_4/\text{SC}$ concentrations (i.e., 4, 6, 8, 10 mM). Offset heights: 5 nm. (b) Plot of adsorbate particle density and V as a function of $\text{Na}_2\text{MoO}_4/\text{SC}$ concentrations (i.e., 4, 6, 8, 10 mM). (c) Offset AFM height profiles of MoS_2 samples prepared from the different $\text{Na}_2\text{MoO}_4/\text{SC}$ concentrations (i.e., 4, 6, 8, 10 mM).

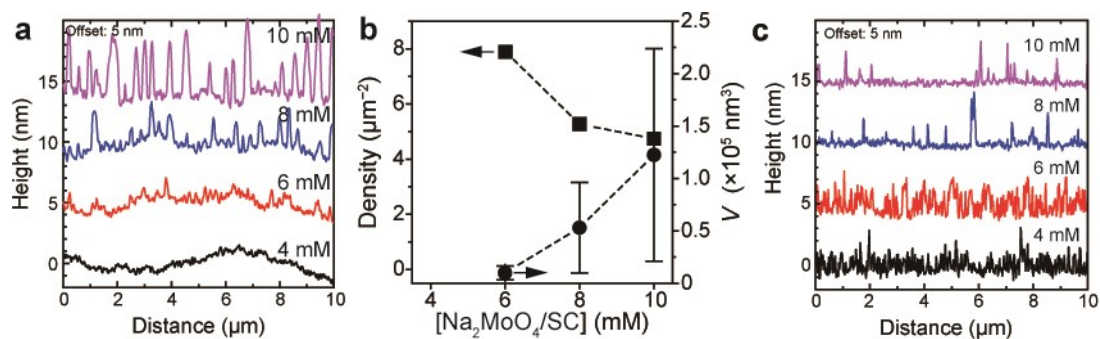


Fig. S3 SEM image and energy dispersive X-ray spectroscopy (EDS). (a) SEM image of continuous MoS₂ film and (b) map of Na K series, (c) map of Mo L series, (d) map of S K series. (e) Atomic percentages of each atom.

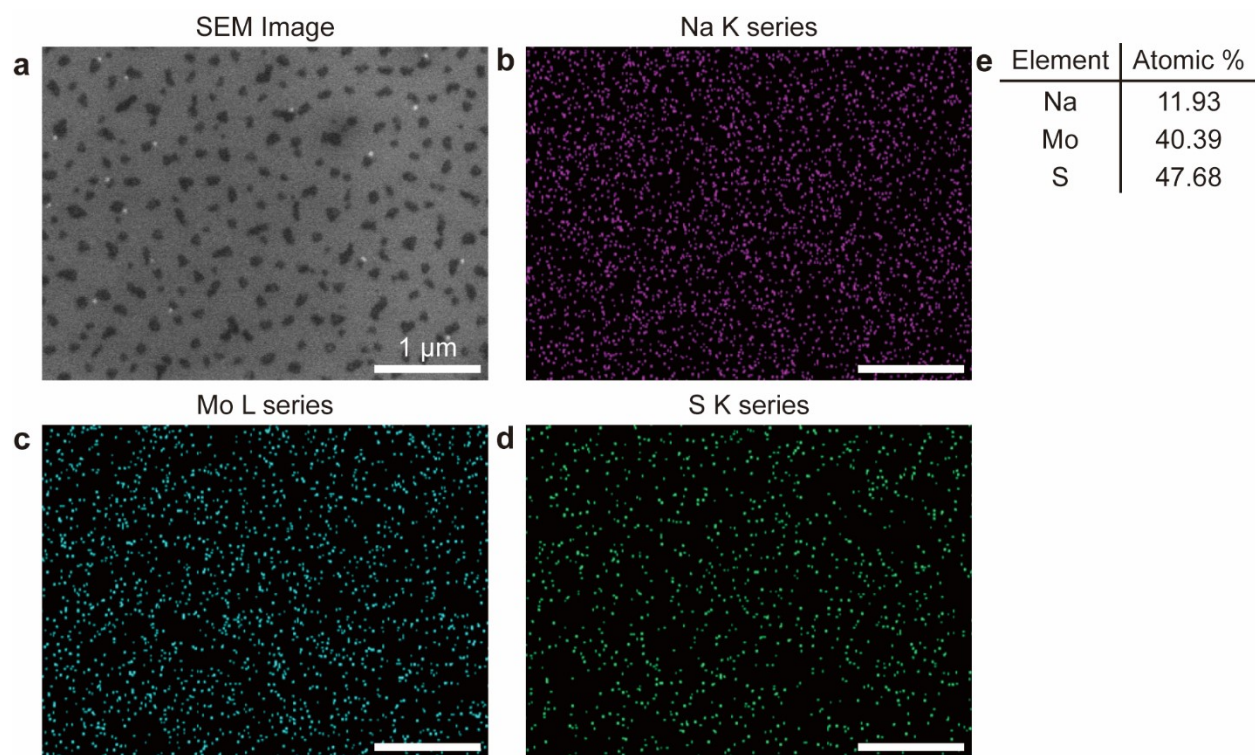


Fig. S4 XPS measurements for the chemical nature of sodium and SC. (a) XPS survey spectra of SC, MoO₃, Na₂MoO₄, Na₂MoO₄/SC drop-cast, and MoS₂ film. Note that the first three are as-received powdery samples, and other two samples are placed on the 285 nm-thick SiO₂/Si substrate. (b–d) XPS detailed spectra of (b) S 2*p*, (c) Mo 3*d*, and (d) Na 1*s* regions.

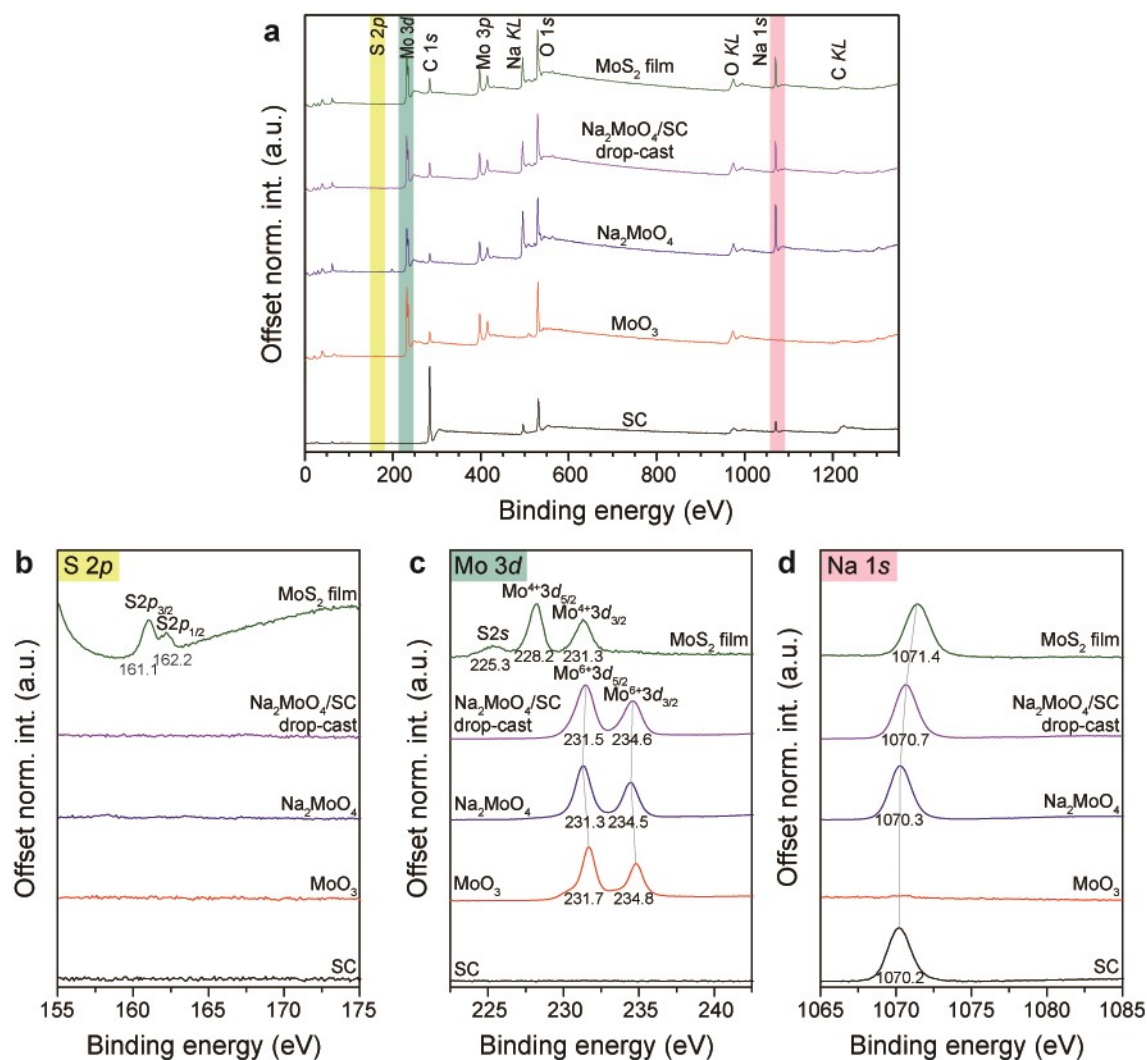


Fig. S5 Attempted MoS₂ growth from a 6 mM MoO₃ dispersion without SC. (a) Profiles of programmed parameters (T_{CVD} , T_{s} , and F_{Ar}) during the ICVDM reaction. The time point corresponding to the optical images is marked. Real-time optical images captured at t_{rxn} = (b) 20 s, (c) 3 min 40 s, and (d) 8 min. (e) C_{R} trends selected positions from (b), plotted as a function of t_{rxn} . (f) Optical image near the interface region after the ICVDM sulfurization. (g) Offset normalized Raman spectra corresponding to the positions in (b). Inset: Zoomed-in Raman spectrum from position 1. Asterisks denote vibrational bands originating from the Si substrate.

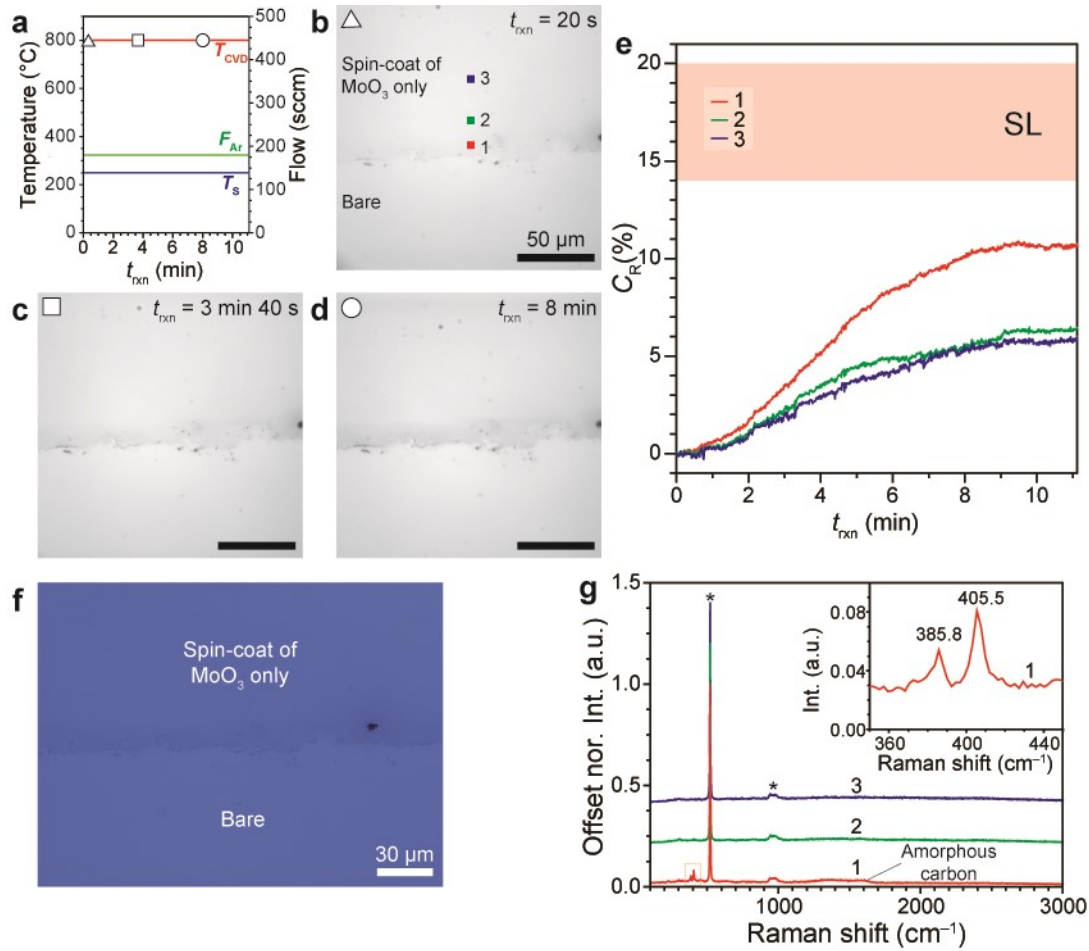


Fig. S6 MoS₂ growth from a 10 mM Na₂MoO₄ dispersion without SC. (a) Profiles of programmed parameters (T_{CVD} , T_{S} , and F_{Ar}) during the ICVDM reaction. The time point corresponding to the optical images is marked. Real-time optical images of MoS₂ film at t_{rxn} = (b) 0 min, (c) 13 min, and (d) 20 min. (e) C_{R} trends selected positions from (b), plotted as a function of t_{rxn} . (f) Optical image near the interface region. Inset: the central region of the spin-coat after the ICVDM sulfurization. (g) Offset normalized Raman spectra corresponding to the positions in (b) and (f). Inset: Raman spectra of MoS₂ vibrational regions in positions 3 and 4. Asterisks indicate the vibrational bands originating from the Si substrate.

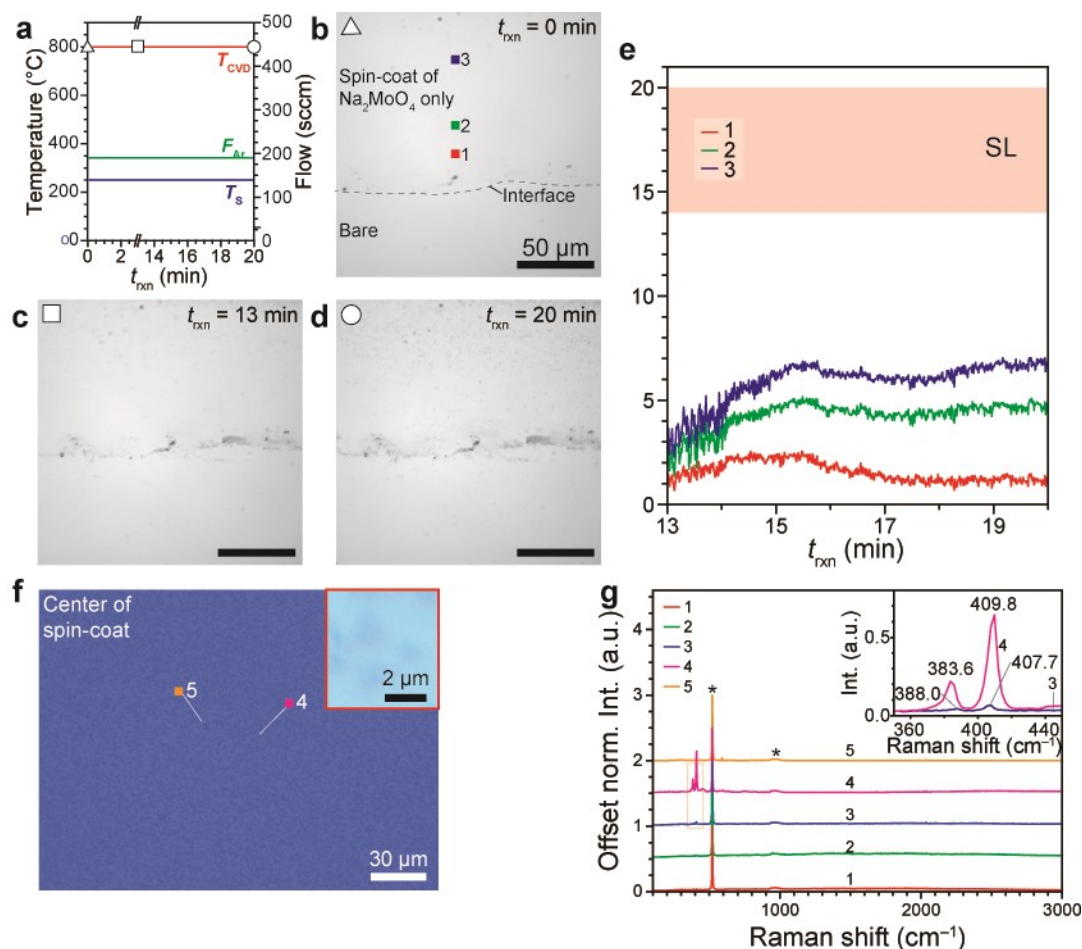
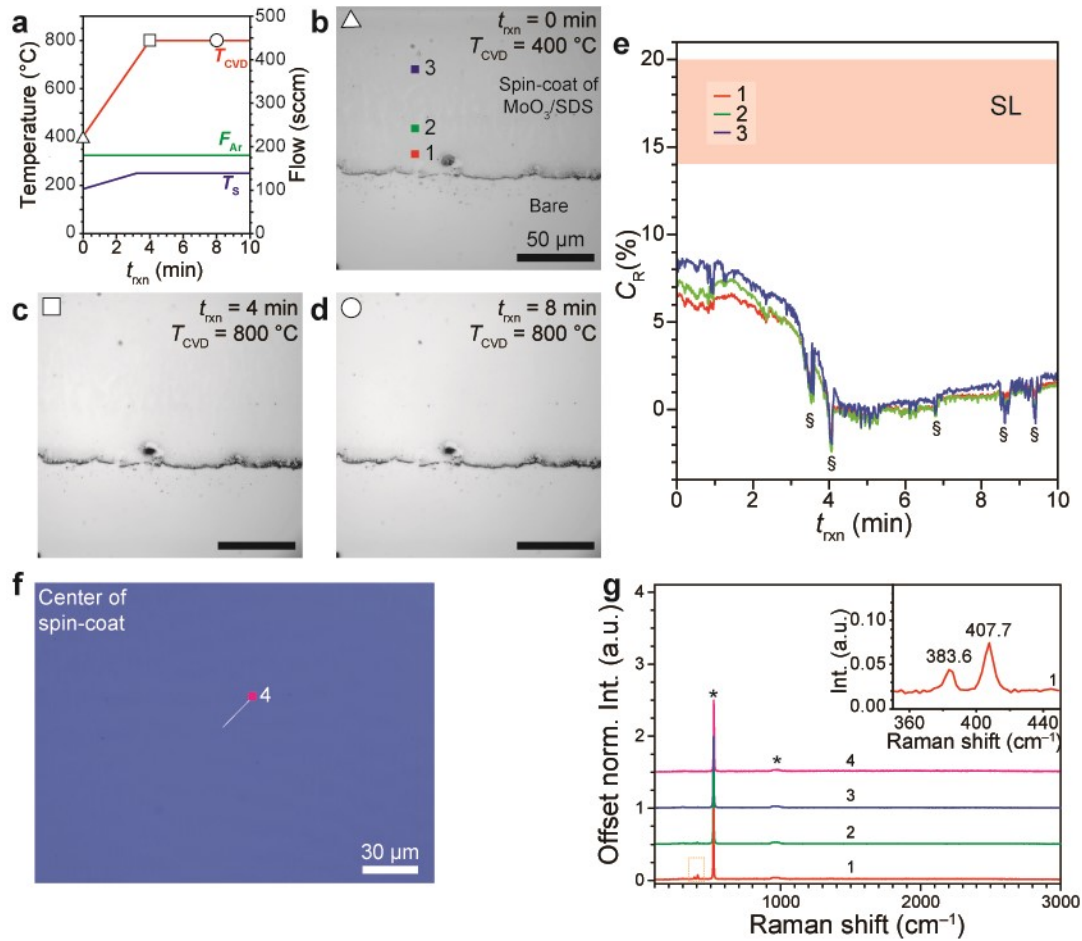


Fig. S7 CVD growth of MoS₂ from the 6 mM MoO₃ dispersion with 1 wt.% SDS. (a) Programming parameter (T_{CVD} , T_{S} , and F_{Ar}) profiles during ICVDM reaction. The t_{rxn} for the optical image is indicated. Real-time optical images of MoS₂ film at t_{rxn} = (b) 0 min, (c) 4 min, and (d) 8 min. (e) C_{R} trends of the positions in the optical images in (b) according to t_{rxn} . Spikes denoted by section sign originate from temporal defocusing. (f) Optical image at the center of the spin-coat. (g) Offset Raman spectra indicated in the optical images in (b) and (f). Inset: Zoomed-in Raman spectrum of position 1. Asterisks denote vibrational bands originating from the Si substrate.



Svideo 1. A movie clip of growing MoS₂ film with spin-coated and bare areas. Conditions: 30 frames per second (fps), 800 °C, 50× magnification.

Cited references

1. M. Jeong, S. Kim and S.-Y. Ju, *RSC Adv.*, 2016, **6**, 36248-36255.
2. G. Eda, H. Yamaguchi, D. Voiry, T. Fujita, M. Chen and M. Chhowalla, *Nano Lett.*, 2011, **11**, 5111-5116.
3. B. V. Crist, Basic XPS Information Section, <https://xpsdatabase.net/sodium-na-z11>, (accessed 2025.05.07.).
4. R. A. Kalt, A. Arcifa, C. Wäckerlin and A. Stemmer, *Nanoscale*, 2023, **15**, 18871-18882.
5. S. Li, Y.-C. Lin, X.-Y. Liu, Z. Hu, J. Wu, H. Nakajima, S. Liu, T. Okazaki, W. Chen, T. Minari, Y. Sakuma, K. Tsukagoshi, K. Suenaga, T. Taniguchi and M. Osada, *Nanoscale*, 2019, **11**, 16122-16129.
6. J. Oh, M. Park, Y. Kang and S.-Y. Ju, *ACS Nano*, 2024, **18**, 19314-19323.